available at www.sciencedirect.com

ScienceDirect

journal homepage: www.ejconline.com

Monitoring the treatment efficacy of the vascular disrupting agent CA4P

Beth A. Salmon[a], *Howard W. Salmon*[b], *Dietmar W. Siemann*[a,c,*]

[a]*Department of Pharmacology and Therapeutics, University of Florida, Gainesville, FL, USA*
[b]*Department of Radiation Oncology, North Florida Cancer Institute, 1021 NW 64th Terrace, Gainesville, FL, USA*
[c]*Department of Radiation Oncology, University of Florida, Box 100385, 2000 SW Archer Road, Gainesville, FL 32610, USA*

ARTICLE INFO

Article history:
Received 19 December 2006
Received in revised form 19 March 2007
Accepted 23 March 2007
Available online 23 April 2007

Keywords:
Vascular targeting
CA4P KHT sarcoma
DCE-MRI
Cytokines

ABSTRACT

The purpose of this study was to investigate two non-invasive methods for determining the treatment efficacy of the vascular disrupting agent (VDA) CA4P: gadolinium enhanced dynamic contrast enhanced magnetic resonance imaging (DCE-MRI) for perfusion analysis and enzyme-linked immunosorbent assay (ELISA) of blood samples. Candidate proteins were identified by multi-analyte profile analysis of plasma from KHT sarcoma-bearing C3H/HeJ mice after CA4P administration. Candidate proteins were further analysed by ELISA of plasma from treated C3H/HeJ, BALBc and C57BL6 mice. Changes in selected proteins, tumour perfusion and tumour necrotic fraction after CA4P treatment were then compared in individual animals. The cytokines KC and MCP-1 were observed to increase after CA4P treatment in all tested models. No correlation was found between KC or MCP-1 levels and tumour necrosis. However, tumour perfusion correlated ($r = 0.89$, $p < 0.00001$) with CA4P treatment efficacy as measured by necrotic fraction, suggesting that DCE-MRI may have utility in a clinical setting.

1. Introduction

Due to the limited diffusion of oxygen and nutrients through tissue, tumours are dependent upon their ability to stimulate angiogenesis (the induction of new blood vessels) in order to grow beyond a size of ~1 mm^3.[1,2] Tumours also must continuously induce angiogenesis as they grow to compensate for the increasing number of cells the vessels must support, resulting in a level of endothelial proliferation not normally found in the adult tissues.[3] The resulting tumour vessels are abnormal in structure, often leaky, tortuous and lacking normal pericyte interaction.[4–7] The presence of these abnormal vessels, which are unique to the tumour, has led to the development of therapeutic strategies aimed at compromising the existing tumour blood vessels.[3]

One class, the vascular disrupting agents (VDAs), which includes Combretastatin A4 Phosphate (CA4P), OXi4503 and ZD6126, targets proliferating endothelial cells by binding tubulin subunits and preventing polymerisation. This results in the depolymerisation of microtubules and reorganisation of the actin cytoskeleton[8] in dividing endothelial cells. Treatment of solid tumours with these VDAs has been shown to lead to tumour vessel occlusion and significantly decreased tumour vascular density.[9–11] Although the precise mechanism of this vessel disruption is not completely understood, the endothelial cell shape changes caused by the reorganisation of the cytoskeleton and disruption of VE-cadherin signalling are believed to play a key role.[12,13] As a result of this tumour vessel disruption, blood flow is significantly reduced to the tumour, and the

* *Corresponding author:* Address: Department of Radiation Oncology, University of Florida, Box 100385, 2000 SW Archer Road, Gainesville, FL 32610, USA.
E-mail address: siemadw@ufl.edu (D.W. Siemann).
0959-8049/$ - see front matter
doi:10.1016/j.ejca.2007.03.018

tumour cells die due to loss of oxygen and nutrient supply.[3,9,14,15]

After VDA treatment, a thin layer of viable tissue survives at the tumour periphery, probably because the cells in this region of the tumour are supported by the normal vasculature which is not disrupted by VDA treatment.[16] These surviving tumour cells can repopulate the tumour, thus limiting the use of these VDAs as a single agent therapy.[17–19] However, these agents effectively destroy regions of the tumour normally resistant to more conventional cancer therapies, raising considerable interest in VDAs as adjuvants to current therapeutic regimens.[10,20,21]

Pre-clinically, VDA efficacy is typically evaluated by analyzing tumour necrotic fraction following treatment. As this method is not practical in the clinical setting, the present study investigated two alternative techniques for monitoring VDA treatment efficacy that could be applied to the clinical setting: blood analysis and gadolinium dynamic contrast enhanced magnetic resonance imaging (DCE-MRI). Proteins involved in the regulation of tissue damage repair released into the plasma as a result of extensive necrosis and tissue damage induced by VDA treatment would be easily examined in a clinical setting by a simple blood test. Potentially, the increase in such proteins might correlate with the extent of tumour damage resulting from VDA treatment. Alternatively, DCE-MRI could be used to visualise the significant reduction in tumour perfusion as a result of VDA treatment. The added advantage of this latter technique is that it has been used on patients receiving VDAs in the clinical setting.[9,11,22] However, to date, there is little evidence to connect a specific change in tumour perfusion, as observed by MRI, to a defined treatment outcome.

In the present study, the microtubule targeting agent CA4P was administered to KHT tumour-bearing mice to identify plasma protein candidates. These candidates were then compared in the individual animal with the laboratory standard marker of treatment efficacy, tumour necrotic fraction, as well as with tumour perfusion as measured by gadolinium DCE-MRI to examine the possibility of correlation with treatment efficacy. The design of this study, therefore, allowed for a direct comparison between plasma proteins, change in tumour perfusion and treatment outcome following CA4P treatment.

2. Materials and methods

2.1. Animals

All research was governed by the principles of the Guide for the Care and Use of Laboratory Animals and approved by the University of Florida Institutional Animal Care and Use Committee (IACUC). C3H/HeJ, BALBc and C57BL6 mice were

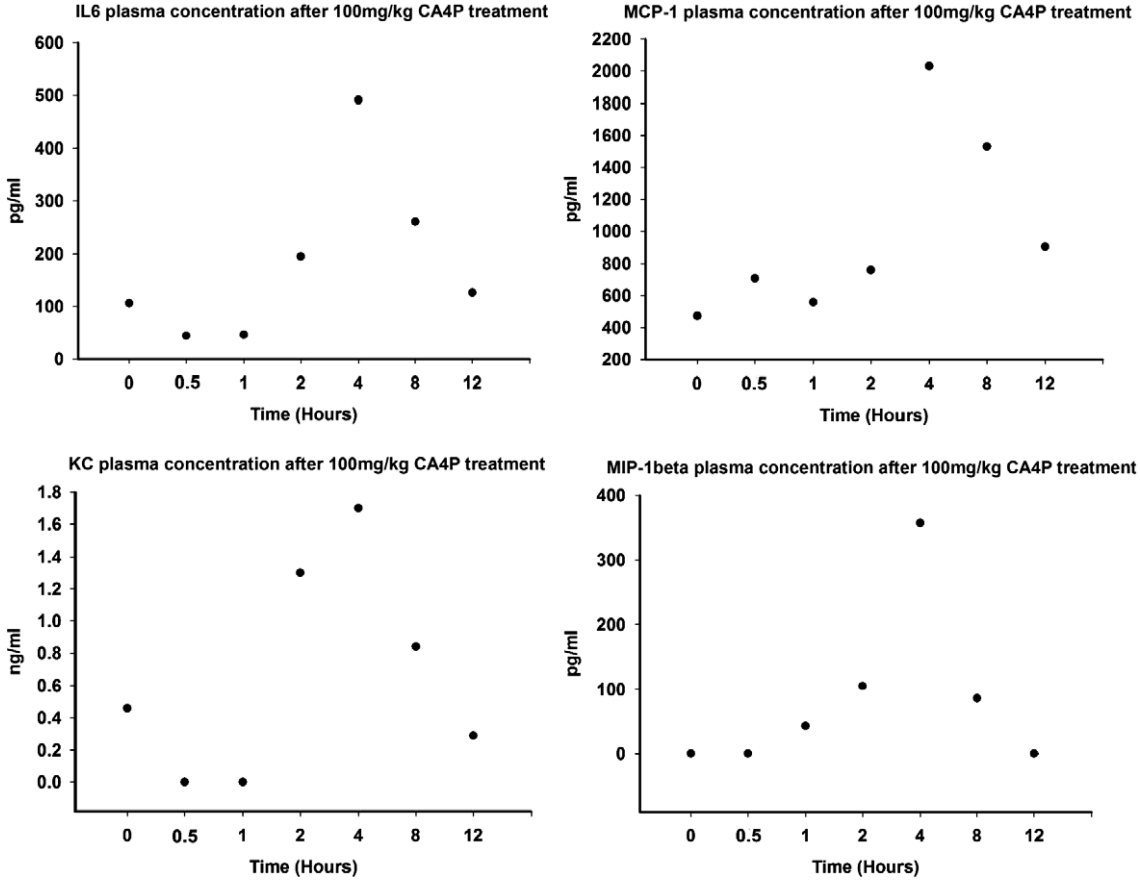

Fig. 1 – MAP results. C3H/HeJ mice-bearing KHT tumours were treated with a single dose of 100 mg/kg CA4P. At various times following treatment, plasma samples were collected and MAPs were obtained to identify changes in plasma protein levels. Each point represents a pooled plasma sample from two mice.

obtained from Jackson Laboratories, Bar Harbor, ME. Mice were 6–8 weeks old and were maintained under a specific pathogen free environment (University of Florida Health Science Center) with food and water *ad libitum*.

2.2. Tumour model

KHT sarcoma cells[23] suspended in PBS were injected intramuscularly in the hind limb of C3H/HeJ mice.[24] The mice were entered into experiments once the tumours reached a size of approximately 300 mm^3.

2.3. Drug preparation and administration

CA4P (OXiGENE Inc., US) was prepared in saline and injected intraperitoneally (IP) at 0.01 ml/g of body weight at a dose of 100 mg/kg. Control animals were injected with saline.

2.4. Identification of candidate proteins

Plasma samples were collected from the tail vein of tumour-bearing C3H/HeJ mice over a 12 h period after treatment with 100 mg/kg CA4P. The plasma from two mice was pooled for each time point ($n = 14$). These samples were then analysed at Charles River Laboratories (Austin, TX) by rodent multi-analyte profiles (MAPs) (designed by Rules Based Medicine, Inc., Austin, TX). Each sample was screened for 80 proteins including cancer markers, cytokines, hormones and those involved in infectious disease.

2.5. Evaluation of selected proteins

Candidate proteins identified by the broad screen were further evaluated by enzyme-linked immunosorbent assay (ELISA) (R&D systems, Minneapolis, MN). Plasma samples from tumour-bearing and non-tumour bearing C3H/HeJ, as well as non-tumour bearing BALBc and C57BL6 mice treated with 100 mg/kg CA4P ($n = 9$) was examined. Blood samples were obtained from the tail vein before and 4 h after VDA administration. To investigate dose response, plasma samples were obtained from KHT tumour-bearing C3H/HeJ mice 4 h after administration of various doses of CA4P (12.5–200 mg/kg) or saline.

2.6. Comparison of methods of establishing treatment efficacy

Pre-treatment plasma samples (Section 2.5) and tumour perfusion measurements (Section 2.7) were obtained from 30

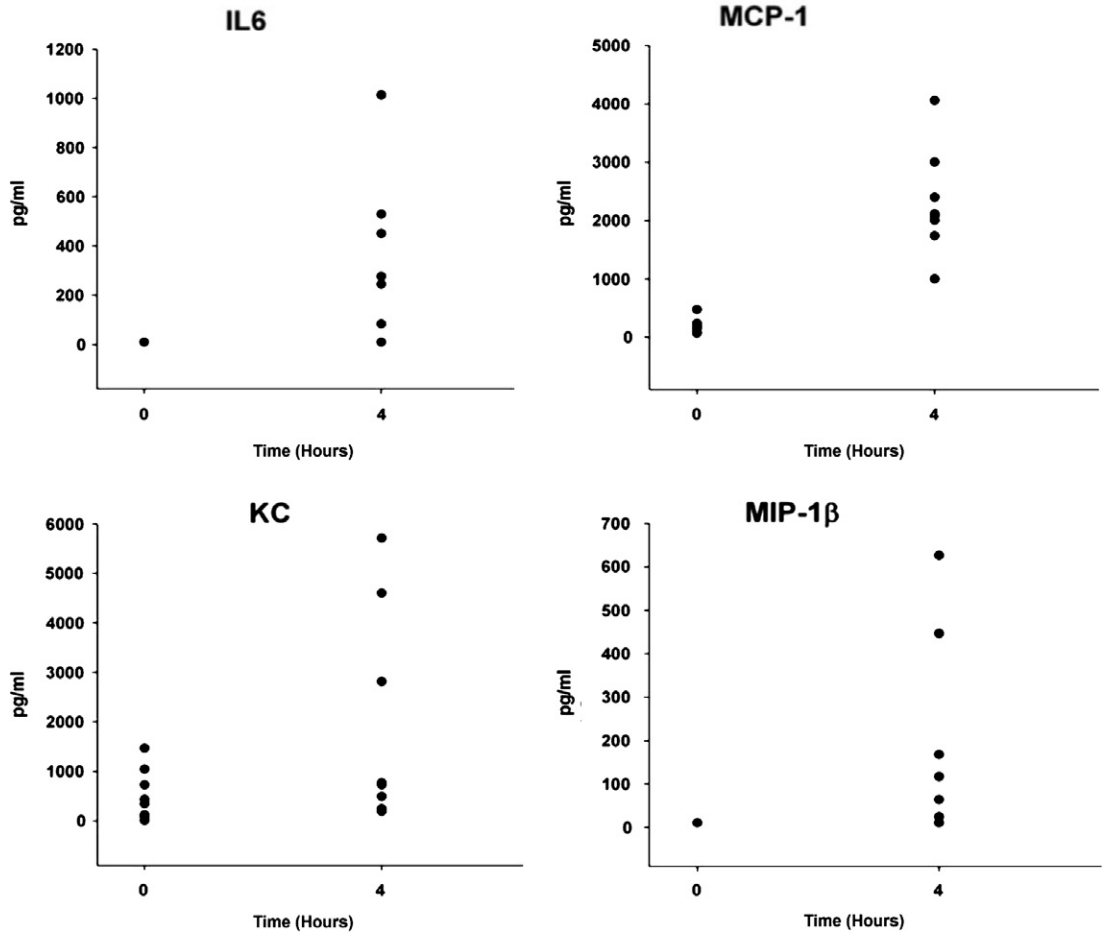

Fig. 2 – CA4P evaluation. Plasma from mice ($n = 8$) bearing KHT tumours was collected before and after treatment with 100 mg/kg CA4P. Data points represent individual animals. As assessed by students *t*-test, MCP-1 $p = 0.0001$, MIP-1β $p = 0.02$, KC $p = 0.1$, and IL6 $p = 0.01$.

C3H/HeJ mice-bearing KHT sarcomas. These data served as a baseline. The following day, the same mice were treated with various doses of CA4P (5–100 mg/kg). Four hours after treatment, plasma samples were again obtained, and tumour perfusion measurements were repeated 1 h later (5 h post treatment). Plasma samples were analysed by ELISA. Twenty-four hours after CA4P administration, the tumours were removed for analysis of tumour necrosis (Section 2.8).

2.7. *Imaging*

The procedures for relative tumour perfusion as well as the evaluation of the dynamic contrast enhanced (DCE) MRI data sets have been described in detail.[25] A brief summary of the methods is given below.

Relative tumour perfusion measurements were determined in tumour-bearing mice using DCE MRI. Contrast-enhanced MRI measurements were made before and 5 h after a single dose treatment of 100 mg/kg CA4P. Images were acquired using a 4.7 T magnet (Oxford Instruments, horizontal boar of 25 cm diameter). The mice were anaesthetised with 2% Isoflurane via induction chamber and maintained with 1.25% Isoflurane via face mask (reducing Isoflurane concentration by 0.25% for every 20 min). A flow of warmed air was used to maintain the body temperature of the animals while in the magnet. Spin-echo images for measurement of relative tumour perfusion were T_1-weighted (TE = 12 ms, TR = 130 ms; field of view 20×20 mm; 128 phase-encode increments and 256 data points, zero-filled to 256×256; 8–14 slices at a slice thickness 1 mm).

Maps of the initial rate of inflow of gadolinium into the tumours were generated by dividing the signal intensity (SI) of the five post contract images acquired 3, 6, 9, 12 and 15 min later, by the SI of the pre contrast image. Changes in relative tumour perfusion were assessed quantitatively by plotting the mean signal intensity in a region of interest defined within central three tumour slices (whole section, excluding skin) against time after bolus injection of 0.2 mmol/kg contrast agent (Omniscan). Relative tumour perfusion was then determined by measuring the integrating area under the signal intensity/time curve.

2.8. *Necrotic fraction*

Twenty-four hours after VDA treatment, tumours were removed and fixed in 10% formalin for 24 h, sectioned and haematoxylin and eosin stained (Molecular Pathology Core, University of Florida). Three sections from each tumour were then imaged by tile field mapping using a morphometric microscope (McKnight Brain Institute, University of Florida). The images were analysed for necrotic fraction by measuring the percent necrotic area over the whole tumour with the analysis software ImageJ. The percent necrosis for each tumour was then determined by averaging the three sections.

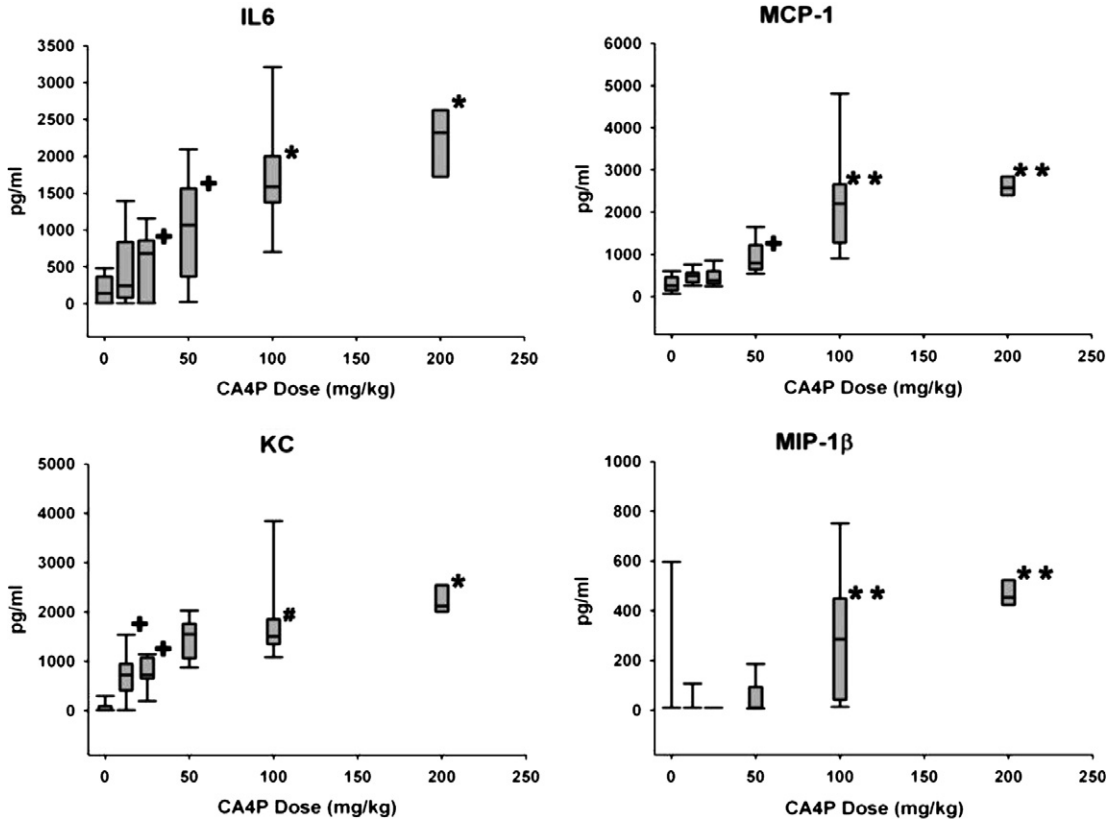

Fig. 3 – CA4P dose response. Mice-bearing KHT tumours were treated with doses of CA4P ranging from 0 to 200 mg/kg. Plasma samples were collected 4 h after treatment and analysed by ELISA. Error bars represent 10th and 90th percentiles, outer box edges represent 25th and 75th percentiles and centre box lines represent median values. (* Significant against all groups, ** significant against 0–50 mg/kg groups, # significant against 0–25 mg/kg groups, + significant against control).

2.9. Statistical analysis

Paired two tailed *t*-tests were performed to establish significance of differences between pre-treatment and post-treatment protein levels using *t*-test analysis. The highest *p*-values are reported. For comparisons between multiple groups, ANOVA and post hoc Scheffe analysis was performed with α set to 0.05. *t*-test, ANOVA and Scheffe analysis were conducted using Microsoft Excel. Correlations were determined by Pearson's Product Moment Correlation Coefficient using Sigmaplot 2001.

3. Results

3.1. Identification of candidate proteins

At various times after CA4P treatment, plasma was collected from tumour-bearing C3H/HeJ mice and proteins were identified through MAP analysis. Compared to untreated mice the levels of four proteins (MCP-1, MIP-1β, KC, IL6) were found to be >2 times higher in plasma from mice examined 4 h after CA4P treatment (Fig. 1). These four cytokines are proteins involved in immune response and wound repair. IL6 is a regulatory protein that is involved in several immune and repair processes, including fever control, monocyte infiltration and reepithelialisation.[26] MCP-1, or macrophage chemoattractant protein, and MIP-1β, macrophage inflammatory protein 1beta, recruit monocytes or macrophages to the site of injury of infection.[26,27] KC is also a chemokine, but is involved in the activation and recruitment of neutrophils.[28]

Subsequent studies used ELISA to confirm plasma protein levels in tumour-bearing C3H/HeJ mice before and after CA4P treatment. Fig. 2 illustrates the observed plasma concentrations in mice treated with a dose of 100 mg/kg CA4P, which indicates a reproducible increase in cytokine concentration after treatment. Mice treated with saline alone showed no significant change (data not shown). To determine the dose dependency of the observed effects, tumour-bearing mice were treated with a range of doses of CA4P and plasma cytokine levels were determined by ELISA. The results showed a dose dependent increase in plasma protein concentration for each of the four tested cytokines (Fig. 3).

3.2. Tumour/host specificity

Non-tumour-bearing C3H/HeJ mice also were treated with CA4P and analysed for plasma cytokine changes (Fig. 4). Such mice were found to express plasma cytokine changes comparable to those obtained in tumour-bearing mice (Fig. 2 versus Fig. 4).

To examine the mouse strain specificity of these effects, non-tumour-bearing BALBc and C57BL6 mice treated with CA4P were also tested. Only two of the candidate proteins, MCP-1 and KC, increased with CA4P treatment in all tested strains (Table 1). As the goal of this study was to identify markers that are likely to be able to be translated into human

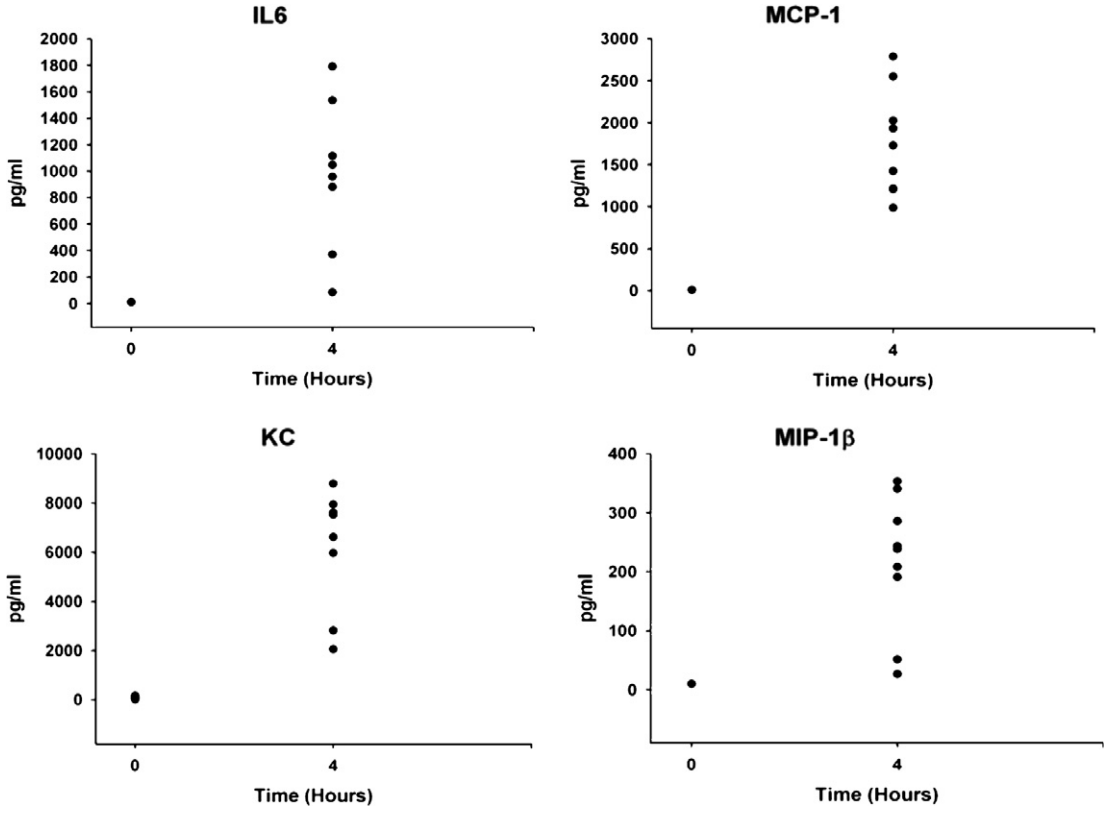

Fig. 4 – Host specificity. Plasma from non-tumour-bearing C3H/HeJ mice was obtained before and after 100 mg/kg CA4P treatment. Samples were analysed by ELISA. Data points represent individual animals. IL6 $p = 0.0002$, KC $p < 0.0001$, MCP-1 $p < 0.0001$, and MIP-1β $p < 0.0001$.

Table 1 – Strain specificity of cytokine response

Strain	Cytokine	Average increase (pg/ml)	Significance
C57BL6	IL6	0.00	
	KC	3004.25	$p < 0.005$
	MCP-1	247.46	$p < 0.05$
	MIP-1β	9.81	
BALBc	IL6	133.67	$p < 0.01$
	KC	3061.51	$p < 0.05$
	MCP-1	354.47	$p < 0.001$
	MIP-1β	0.00	

testing, the proteins IL6 and MIP-1β were excluded from further study as they failed to demonstrate a consistent response across the tested strains.

3.3. *Comparison of VDA treatment response end-points in individual mice*

Necrotic fraction (an established end-point for VDA treatment efficacy) and change in cytokines and tumour perfusion were determined for each animal following CA4P exposure. These parameters were then compared for possible correlations. Using this approach, neither KC nor MCP-1 levels correlated with necrotic fraction (Fig. 5). Cytokine changes also did not relate to changes in tumour perfusion as measured by DCE-MRI (Fig. 6). However, when changes in tumour perfusion were compared to the tumour necrotic fraction, a significant correlation emerged (Pearson's correlation coefficient 0.89, $p < 0.00001$) (Fig. 7). Larger changes in tumour perfusion corresponded with larger necrotic fraction values, while smaller perfusion changes resulted in lesser necrotic fraction values following CA4P treatment.

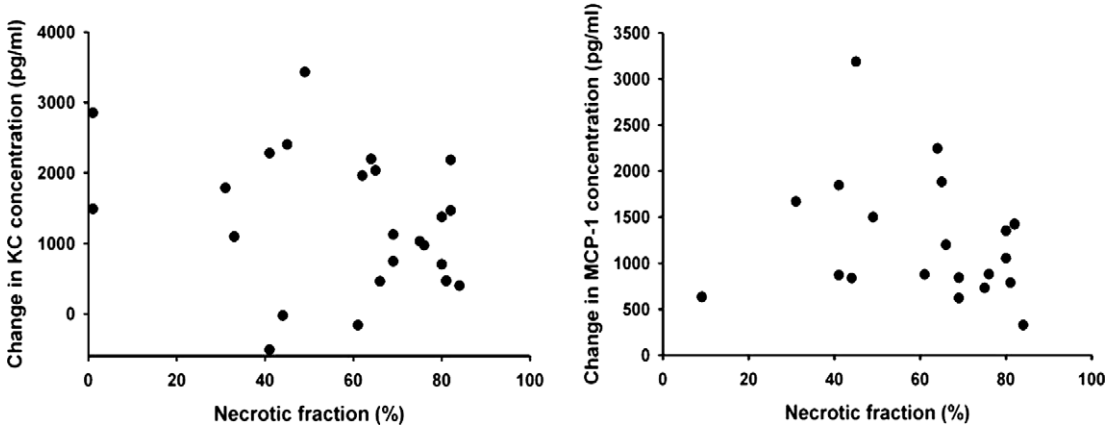

Fig. 5 – Comparison of cytokine concentration change and necrotic fraction in individual mice treated with CA4P. Plasma from mice-bearing KHT tumours was collected before and 4 h after 25 or 100 mg/kg CA4P treatment. ELISAs were performed to establish protein levels. Twenty-four hours after treatment, the tumours were removed and necrotic fraction was determined. The change in cytokine concentration for each mouse was then paired with its tumour's observed necrotic fraction. Data points represent individual animals.

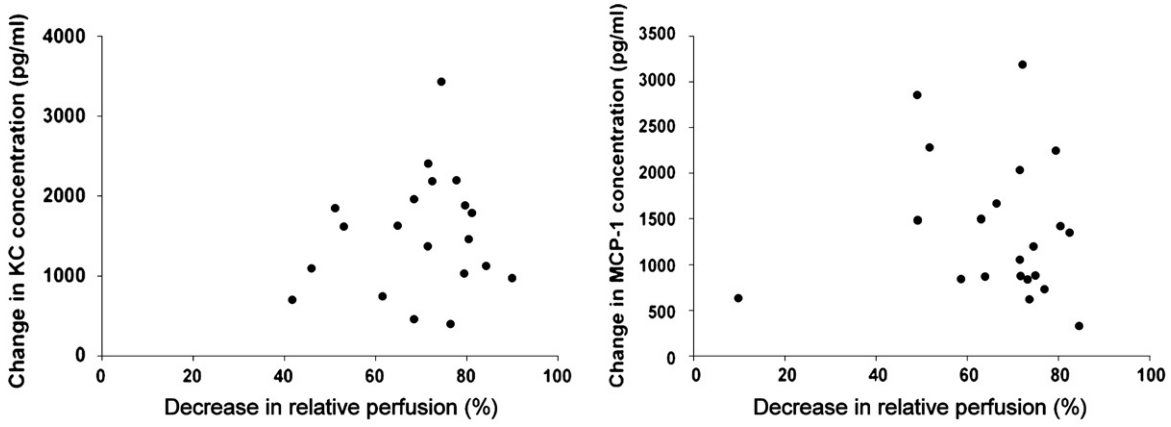

Fig. 6 – Comparison of cytokine concentration change and perfusion in individual mice treated with CA4P. The tumours from the mice from the experiment depicted in Fig. 5 were also imaged using gadolinium DCE-MRI before and 5 h after 25 or 100 mg/kg CA4P treatment. The change in cytokine concentration for each mouse was then compared with its tumour's observed change in perfusion. Data points represent individual animals.

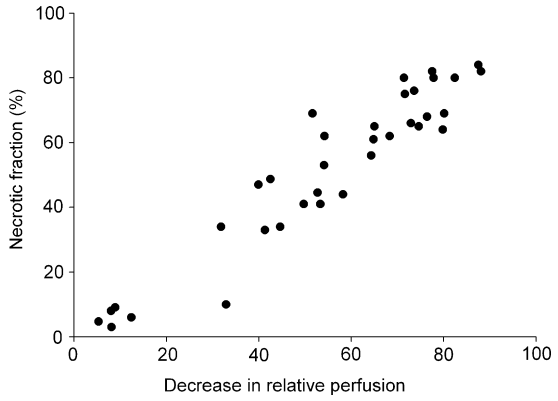

Fig. 7 – Comparison of decrease in relative perfusion and necrotic fraction in individual mice treated with CA4P. Data points represent individual animals. $r = 0.89$, $p < 0.00001$.

4. Discussion

VDAs offer a potentially attractive therapy for application in combination with conventional cancer treatments due to their effective destruction of microenvironmental regions of the tumour typically resistant to conventional anticancer therapies. Several clinical trials combining VDAs with chemotherapy or radiotherapy[21] are currently underway. Pre-clinical evaluations of VDA treatment have typically assessed the percentage of induced tumour necrosis as a measure of their efficacy, but such evaluations are not readily applicable to the clinical setting. The aim of this study, therefore, was to evaluate two alternative potential markers for monitoring VDA treatment efficacy; plasma proteins as measured by ELISA and tumour perfusion as determined by gadolinium DCE-MRI. These potential markers were all analysed in the same animal after CA4P treatment, allowing for direct comparisons between the surrogate markers and treatment outcome as determined by tumour necrotic fraction.

The results showed a significant cytokine response to CA4P treatment. The proteins KC, MIP-1β IL6 and MCP-1 were observed to consistently increase in the plasma of mice 4 h after treatment. A dose dependent increase in cytokine concentration was observed with increasing CA4P treatment, indicating a specific response to this VDA. Non-tumour-bearing mice also displayed the cytokine increase in response to CA4P, suggesting that the observed cytokine elevation reflected a host response rather than being a result of tumour damage. Interestingly, two of the four cytokines, IL6 and KC, are chemokines involved in neutrophil activation; a finding that may relate to the increase in neutrophils that has been observed in solid tumours following VDA treatment.[29] Parenthetically, increased neutrophil infiltration also has been reported in tumours of patients undergoing CA4P treatment (Chaplin, D., personal communication, 2005).

Despite the lack of a direct tumour specific effect, it may be argued that if the observed cytokine increases occurred in a manner paralleling the extents of CA4P-induced tumour damage, changes in host cytokine production might still be useful as a surrogate marker of treatment efficacy. Such an outcome would suggest that cytokine measurements in plasma of patients undergoing CA4P therapy might offer important information regarding CA4P dosing. Unfortunately, this was not born out in the experimental studies. Indeed increases in plasma concentration of either KC or MCP-1, the cytokines found to be elevated in all three mouse strains following CA4P exposure, failed to correlate with treatment outcome as determined by tumour necrotic fraction measurement (Fig. 5).

Somewhat surprising in these studies was the absence of an elevation of plasma VEGF in the initial broad screen analysis of KHT tumour-bearing mice following CA4P administration. This result was in contrast to a recent study which demonstrated significant VEGF increases following treatment of MHEC5-T tumours[30] with a related VDA (OXi4503). However, immunohistochemical analysis of KHT tumours also failed to demonstrate significant changes in VEGF expression following CA4P treatment (data not shown). Still, the focus on the four chosen proteins in the present study does not preclude the variations in plasma concentrations of other cytokines nor does the broad screen MAP analysis necessarily indicate their non-involvement in either the tumour or host response to VDA treatment.

Post-treatment increases in the evaluated cytokines have not previously been reported for the tubulin binding VDAs. Indeed previous *in vitro* evaluations of cytokine levels in cell lines following VDA administration failed to identify a significant effect of combretastatin VDAs on cytokine expression.[10] The *in vivo* results reported here suggest that the cytokine responses reflect a direct host reaction to CA4P exposure. Further studies investigating the source of the cytokine production and the aspects of VDA action that could induce this normal tissue response are clearly warranted.

Results of the MRI experiments reveal a significant correlation between tumour perfusion and necrotic fraction following VDA treatment, supporting the findings of the previously published study relating these parameters.[25] However, unlike the previously published study which compared the response of groups of animals, the current study demonstrates a relationship between tumour perfusion and tumour necrosis in individual mice.

In summary, while changes in KC and MCP-1 cytokine concentrations were observed across three mouse strains, no direct correlation could be established between cytokine concentration changes and either tumour necrotic fraction or DCE MRI based tumour perfusion. In contrast, CA4P-induced tumour necrosis assessments and DCE MRI based tumour perfusion measurements did show a significant correlation, supporting the continued use of this non-invasive imaging technique for the monitoring of patient treatment efficacy after CA4P administration. Given the availability of MRI in most hospitals, the application of this approach in clinical evaluations of VDA therapy is highly feasible.

Conflict of interest statement

D.W. Siemann serves on the scientific advisory board of OXiGENE, Inc.

Acknowledgements

This work was supported by USPHS grant CA-84408. The authors gratefully acknowledge the Optical Microscopy Facility and the Advanced Magnetic Resonance Imaging and Spectroscopy Facility, Evelyn F. & William L. McKnight Brain Institute of the University of Florida, Gainesville, Florida, in the performance of these studies. CA4P was provided by OXiGENE, Waltham, MA 02451, USA.

REFERENCES

1. Folkman J. How is blood-vessel growth regulated in normal and neoplastic tissue – Gha Clowes Memorial Award Lecture. *Cancer Res* 1986;**46**:467–73.
2. Ausprunk DH, Folkman J. Migration and proliferation of endothelial cells in preformed and newly formed blood-vessels during tumor angiogenesis. *Microvascu Res* 1977;**14**:53–65.
3. Denekamp J. Vascular attack as a therapeutic strategy for cancer. *Cancer Metast Rev* 1990;**9**:267–82.
4. Tozer GM, Kanthou C, Baguley BC. Disrupting tumour blood vessels. *Nat Rev Cancer* 2005;**5**:423–35.
5. Hashizume H, Baluk P, Morikawa S, et al. Openings between defective endothelial cells explain tumor vessel leakiness. *Am J Pathol* 2000;**156**:1363–80.
6. Morikawa S, Baluk P, Kaidoh T, Haskell A, Jain RK, McDonald DM. Abnormalities in pericytes on blood vessels and endothelial sprouts in tumors. *Am J Pathol* 2002;**160**:985–1000.
7. Baluk P, Morikawa S, Haskell A, Mancuso M, McDonald DM. Abnormalities of basement membrane on blood vessels and endothelial sprouts in tumors. *Am J Pathol* 2003;**163**:1801–15.
8. Kanthou C, Tozer GM. The tumor vascular targeting agent combretastatin A-4-phosphate induces reorganization of the actin cytoskeleton and early membrane blebbing in human endothelial cells. *Blood* 2002;**99**:2060–9.
9. Thorpe PE. Vascular targeting agents as cancer therapeutics. *Clin Cancer Res* 2004;**10**:415–27.
10. Tozer GM, Kanthou C, Parkins CS, Hill SA. The biology of the combretastatins as tumour vascular targeting agents. *Int J Exp Pathol* 2002;**83**:21–38.
11. Gaya AM, Rustin GJ. Vascular disrupting agents: a new class of drug in cancer therapy. *Clin Oncol* 2005;**17**:277–90.
12. Galbraith SM, Chaplin DJ, Lee F, et al. Effects of combretastatin A4 phosphate on endothelial cell morphology in vitro and relationship to tumour vascular targeting activity in vivo. *Anticancer Res* 2001;**21**:93–102.
13. Vincent L, Kermani P, Young LM, et al. Combretastatin A4 phosphate induces rapid regression of tumor neovessels and growth through interference with vascular endothelial-cadherin signaling. *J Clin Invest* 2005;**115**:2992–3006.
14. Siemann DW. Vascular targeting agents: an introduction. *Int J Radiat Oncol Biol Phys* 2002;**54**:1472.
15. Chaplin DJ, Dougherty GJ. Tumour vasculature as a target for cancer therapy. *Br J Cancer* 1999;**80**(Suppl. 1):57–64.
16. Siemann DW. Vascular targeting agents. *Horizons Cancer Ther* 2002;**3**:4–15.
17. Dark GG, Hill SA, Prise VE, Tozer GM, Pettit GR, Chaplin DJ. Combretastatin A-4, an agent that displays potent and selective toxicity toward tumor vasculature. *Cancer Res* 1997;**57**:1829–34.
18. Lash CJ, Li AE, Rutland M, Baguley BC, Zwi LJ, Wilson WR. Enhancement of the anti-tumour effects of the antivascular agent 5,6-dimethylxanthenone-4-acetic acid (DMXAA) by combination with 5-hydroxytryptamine and bioreductive drugs. *Br J Cancer* 1998;**78**:439–45.
19. Rojiani AM, Li L, Rise L, Siemann DW. Activity of the vascular targeting agent combretastatin A-4 disodium phosphate in a xenograft model of AIDS-associated Kaposi's sarcoma. *Acta Oncol* 2002;**41**:98–105.
20. Horsman MR, Murata R. Vascular targeting effects of ZD6126 in a C3H mouse mammary carcinoma and the enhancement of radiation response. *Int J Radiat Oncol Biol Phys* 2003;**57**:1047–55.
21. Siemann DW, Chaplin DJ, Horsman MR. Vascular-targeting therapies for treatment of malignant disease. *Cancer* 2004;**100**:2491–9.
22. Galbraith SM, Maxwell RJ, Lodge MA, et al. Combretastatin A4 phosphate has tumor antivascular activity in rat and man as demonstrated by dynamic magnetic resonance imaging. *J Clin Oncol* 2003;**21**:2831–42.
23. Kallman RF, Silini G, Van Putten LM. Factors influencing the quantitative estimation of the in vivo survival of cells from solid tumors. *J Natl Cancer Inst* 1967;**39**:539–49.
24. Siemann DW, Rojiani AM. The vascular disrupting agent ZD6126 shows increased antitumor efficacy and enhanced radiation response in large, advanced tumors. *Int J Radiat Oncol Biol Phys* 2005;**62**:846–53.
25. Salmon HW, Siemann DW. Effect of the second-generation vascular disrupting agent OXi4503 on tumor vascularity. *Clin Cancer Res* 2006;**12**:4090–4.
26. Werner S, Grose R. Regulation of wound healing by growth factors and cytokines. *Physiol Rev* 2003;**83**:835–70.
27. Schall TJ, Bacon K, Camp RD, Kaspari JW, Goeddel DV. Human macrophage inflammatory protein alpha (MIP-1 alpha) and MIP-1 beta chemokines attract distinct populations of lymphocytes. *J Exp Med* 1993;**177**:1821–6.
28. Bacon KB, Oppenheim JJ. Chemokines in disease models and pathogenesis. *Cytokine Growth Fact Rev* 1998;**9**:167–73.
29. Parkins CS, Holder AL, Hill SA, Chaplin DJ, Tozer GM. Determinants of anti-vascular action by combretastatin A-4 phosphate: role of nitric oxide. *Br J Cancer* 2000;**83**:811–6.
30. Sheng Y, Hua J, Pinney KG, et al. Combretastatin family member OXI4503 induces tumor vascular collapse through the induction of endothelial apoptosis. *Int J Cancer* 2004;**111**:604–10.